

---

Article

# Adsorption of hexavalent chromium by sodium alginate fiber biochar loaded with lanthanum

Xinzhe Sun<sup>1</sup>, Peng Guo<sup>2</sup>, Yuanyuan Sun<sup>3,\*</sup> and Yuqian Cui<sup>1,\*</sup>

<sup>1</sup> College of Environmental Science and Engineering, Qingdao University, Qingdao 266071, China; sxz19960916@163.com

<sup>2</sup> School of Chemical Engineering, China University of Petroleum (East China), Qingdao 266580, China; guopeng@upc.edu.cn

<sup>3</sup> School of Environmental Science and Engineering, State Key Laboratory of Bio-Fibers and Eco-Textiles, Shandong Collaborative Innovation Center of Marine Bio-Based Fibers and Ecological Textiles, Qingdao University, Qingdao, 266071, China

\* Correspondence: bonnie\_cyq@163.com (Y.C); sunyuan870102@163.com (Y.S); Tel.: +86 13793235399 (Y.C); +86 15264230805 (Y.S)

**Abstract:** Lanthanum chemical compound incorporates a sensible anionic complexing ability, however lacks stability at low pH scale. Biochar fibers will benefit of their massive space and plethoric useful teams on surface to support metal chemical compound. Herein, wet spinning technology was used to load La<sup>3+</sup> onto sodium alginate fiber, and convert La<sup>3+</sup> into La<sub>2</sub>O<sub>3</sub> through carbonization. The La<sub>2</sub>O<sub>3</sub> modified biochar (La-BC) fiber was characterized by SEM, XRD and XPS, etc. The adsorption experiment proved that La-BC showed excellent adsorption capacity for chromates, and its saturation adsorption capacity was about 104.9mg/g. The information suggested that the adsorption was in step with both Langmuir and Freundlich model, followed pseudo-second-order surface assimilation mechanics, which instructed that the Cr (VI) adsorption was characterized by single-phase and polyphase adsorption, mainly chemical adsorption. Thermodynamic parameter proved that the adsorption process was spontaneous and endothermic. The mechanistic investigation revealed that the mechanism of adsorption of Cr (VI) by La-BC may include electrostatic interaction, ligand exchange or complexation. Moreover, co-existing anions and regeneration experiments proved that La-BC was recyclable and had a good prospect in the field of chrome-containing wastewater removal.

**Keywords:** Wet spinning; Lanthanum oxide; Biochar; Chromate; Adsorption

---

## 1. Introduction

Chromium (Cr) is one amongst the foremost typical and venomous significant metal ions, which is widely found in wastewater from a variety of industries, such as textiles, metallurgy, metal electroplating, and tanneries[1]. Chromium can cause serious environmental problems and harm human health due to its problem characteristics of bio-accumulation, non-biodegradability and potential carcinogenicity in the food chain[2, 3].

Generally speaking, chromium in nature mainly exists in 2 stable states in a wide pH range: trivalent chromium (Cr (III)) and hexavalent chromium (Cr (VI)). Cr (III) is non-toxic and can be effectively removed by precipitation (such as chromium hydroxide) or adsorption[4-7]. Cr (VI) are more dangerous because they have toxicity, higher solubility and mobility[4]. It appears in forms of chromate (CrO<sub>4</sub><sup>2-</sup>, HCrO<sub>4</sub><sup>-</sup>) and dichromate (Cr<sub>2</sub>O<sub>7</sub><sup>2-</sup>), which has caused great environmental concern[3, 8]. As a priority toxic pollutant identified by the US environmental protection agency, Cr (VI) can cause serious toxic and detrimental effects on human health and ecosystems. When the Cr (VI) content in drinking water exceeds 0.05 mg/L and that in water for different uses exceeds 0.1 mg/L, it can cause harm to human health, such as kidney, liver and stomach damage, skin allergy and lung cancer[9], but in contaminated natural water and industrial waste water, Cr (VI)

tends to be more than 200 mg/L[10, 11]. Therefore, practical methods must be developed to remove Cr (VI), to protect the aquatic environment.

Compared with the strategies such as membrane separation, biodegradation, electrochemical oxidation, solvent extraction and other treatment methods, capture of Cr (VI) using adsorbing media has numerous advantages such as non-toxic and harmless process, easy operation, versatility and low cost[12-14]. The adsorbents with different sites will interact with Cr (VI) through different mechanism including direct precipitation, electrostatic interaction, ligand exchange, intra sphere complexation and redox[1, 15-17]. Many of naturally available adsorbents such as sawdust, pine needles and seaweed have the disadvantages of low adsorption capacity and slow adsorption process. Thus, to realize the unification of economic and environmental benefits, there is a need to create innovative and economical adsorbents for composite materials with high efficiency[18].

Biochar (BC) has recently received significant attention because of its beneficial surface physical/chemical properties for the removal of heavy metals from wastewater[19-21]. However, the surface of the original BC is usually negatively charged with low ability of anion removal. Rare earth metal oxides can participate in chemical reactions as active components, and have been widely used in petroleum, metallurgy, ceramics, textiles and other fields. Lanthanum oxide ( $\text{La}_2\text{O}_3$ ) has good anionic complexation ability, but lacks stability under low pH conditions. Actually, biochar fibers can take advantage of their large surface area and abundant surface functional groups to support lanthanum oxide, meanwhile, pores in biochar could enhance the dispersion of La and improve the consumption efficiency, so biochar is a viable option to support La incorporation[22]. Recently, biochar materials with lanthanum oxide doped have been extensively studied and exhibit several advantages in removing oxygen-containing acids, such as strong adsorption selectivity, remarkable adsorption capacity, high removal rate and wide pH range. According to Yang Bei (2019), through inner-sphere complexation, La-doped biochar can form La-O-P chemical bond with phosphate to remove  $\text{PO}_4^{3-}$  in sewage[23], while Haiyang Yang(2019) stated that Cr (VI) adsorption might be related to the outer-sphere complexation. Therefore, we speculate that chromate can also bond with La-BC with the same chemical bond[24, 25]. In addition, other literature data shows that lanthanum containing materials have an excellent effect on the removal of phosphate, antimonate and arsenate in water[14, 21, 26-31]. As a great biochar doping component, La can improve the adsorption capacity of anions. But there are few reports in the literature on the use of La doped BC to remove Cr (VI). Moreover, the adsorption capacity of Cr (VI) by La-based adsorbents is also low in these relevant literatures. For example, the adsorption capacity of hexavalent chromium in chitosan and lanthanum mixed oxyhydroxide is only 48.3mg/g[32]. To investigate the adsorption capacity of La to chromate, a lanthanum oxide loaded carbon fiber material was prepared by calcination at 900°C. By using La-BC, Cr (VI) can be effectively removed. The possible mechanism is discussed in detail. It is proved that the adsorption effect of La-BC on Cr (VI) is better than that of other La-based adsorbents reported in literature. Beyond that, La-BC is recyclable and has a good prospect in the field of chrome-containing wastewater removal.

## 2. Materials and Methods

### 2.1. Materials

The reagents included lanthanum chloride, sodium alginate (alighting), potassium dichromate, hydrochloric acid, sodium hydroxide, sulfuric acid, phosphoric acid, sodium chloride, sodium sulfate, sodium nitrate, sodium bicarbonate, disodium phosphate, acetone, and diphenylcarbazine. All chemicals and reagents were analytical pure, produced by sinopharmaceutical chemical reagent co., LTD., except sodium alginate(AR, Shanghai Aladdin Bio-Chem Technology Co., LTD). All solutions were prepared using deionized water.

### 2.2. Preparation of adsorbent

La<sup>3+</sup> loaded sodium alginate fiber (La-SA) was prepared by wet spinning with 4% sodium alginate solution as spinning solution and lanthanum chloride (LaCl<sub>3</sub>) solution with the same concentration as coagulate bath. La-SA was placed in an oven at 30°C and dried for 24 hours. The dried La-SA was transferred to a tube furnace and pyrolyzed at 900°C for 1h (with a heating rate of 5°C/min). After ground and sifted, the biochar (La-BC) loaded with lanthanum oxide (La<sub>2</sub>O<sub>3</sub>) was obtained for the experiment.

### 2.3. Characterization

The Brunauer-Emmett-Teller equation was used to determine the specific surface area while the pore structures were calculated by nitrogen adsorption/desorption isotherms carried out on a surface area and porosity analyzer (3H-2000PS2, China). The surface morphology of material was observed by scanning electron microscopy (SEM, SU8020, Japan). Besides, the phase structure of materials was examined by X-ray diffraction (XRD, DX2700, China) at a scan rate (2θ) of 6°/min from 10° to 80° and an accelerating voltage of 40 kV. X-ray photoelectron spectroscopy (XPS, ULTRAESCALAB 250Xi, USA) was used to analyze the surface functional groups and the valence state of chromium with monochromatic 150 WAl Kα radiation.

### 2.4. Adsorption and desorption experiments

A series of adsorption and desorption experiments were carried out to evaluate the adsorption properties of La-BC and analyze its adsorption mechanism. Potassium dichromate (2.827g) was dissolved in distilled water (1000mL) to make a 1000mg/L dichromate stock. Then the stock was diluted to produce dichromate solutions of different concentrations. The effects of carbonization temperature (700-1000°C), solution pH (2-10), adsorption isotherm (initial concentration 20-1000mg/L), adsorption kinetics (shaken for 3h in oscillator), adsorption thermodynamics (adsorbent temperature 298-318K) and co-existing acid ions on the adsorption of Cr (VI) were analyzed in turn. In order to assess the reusability of La-BC as Cr (VI) adsorbent, five adsorption/desorption cycles were conducted. The filtrate was filtered with a 0.45μm nylon membrane syringe after adsorption. The clear solution was extracted and the possible leaching concentrations of Cr<sup>6+</sup> and La<sup>3+</sup> in the adsorbed solution were determined by visible light spectrophotometer and inductively coupled plasma emission spectrometer respectively.

In all the adsorption experiments, the dosage of La-BC was 1g/L. The pH of all solutions was not adjusted separately except for the pH experiment. Similarly, all experiments were conducted at room temperature (298K or 303K), except the adsorption thermodynamics experiment. Due to the indoor temperature difference in different seasons, the specific experimental conditions are described in detail in the results and discussion section below. In addition, in all the charts in this paper, the data involving Cr(VI) content such as Cr(VI) solution concentration and adsorption capacity, were calculated by total Cr<sup>6+</sup> content.

## 3. Results and Discussion

### 3.1. Characterization of La-BC

Table S1 shows some of the physical properties of carbonized adsorbents at different temperatures. According to the nitrogen adsorption-desorption curve (Figure S1), it can be found that all the four carbon adsorbents are type IV with H4 hysteresis loop, indicating that the lanthanum supported biochar through high temperature carbonization is a mesoporous material [28, 33]. The specific surface area and porosity of the adsorbent have important influence on its adsorption capacity [20, 34]. Generally speaking, the larger the specific surface area is, the more adsorption points are available, and the larger the adsorption capacity will be. The specific surface area of La-BC (900°C) reached 177.41 m<sup>2</sup>/g, while the specific surface areas of La-BC (700°C), La-BC (800°C) and La-BC (1000°C) were 8.21m<sup>2</sup>/g, 38.61m<sup>2</sup>/g and 52.08m<sup>2</sup>/g respectively, indicating that La-BC (900°C) might

be the adsorbent with the highest adsorption capacity. In addition, by comparing the pore volume, it was found that the pore volume of La-BC (900°C) was 0.2515cm<sup>3</sup>/g, which was larger than the other three adsorbents. Larger pore volume also facilitates the adsorption of target elements.

SEM images, TEM images and element mapping were used to research and analyze the surface morphology and element distribution of La-BC (900°C) (Figure 1). As a porous material, biochar is a good substrate for lanthanum deposition. The sodium alginate biochar supported by lanthanum was fibrous, with a diameter of about 20-50µm. The surface was rough and irregular with a large number of acicular crystals and loose pores distributed (Figure 1a, b and c). The same morphology was also shown in TEM images, in which the fractured biochar fibers were supported by needle-like or rod-like crystals ((Figure 1d, e and f). The lattice fringe of La-BC can be observed more clearly through the analysis of the high-resolution TEM image (Figure 1g). Compared with the standard card La<sub>2</sub>O<sub>3</sub> (PDF#05-0602), the lattice spacing of 0.335nm and 0.346nm both correspond to the (100) plane of La<sub>2</sub>O<sub>3</sub>. Through the SEM-EDS element mapping image of La-BC (900°C), La element can be observed evenly (Figure 1h), proving that La element has been successfully loaded on the surface of biochar.

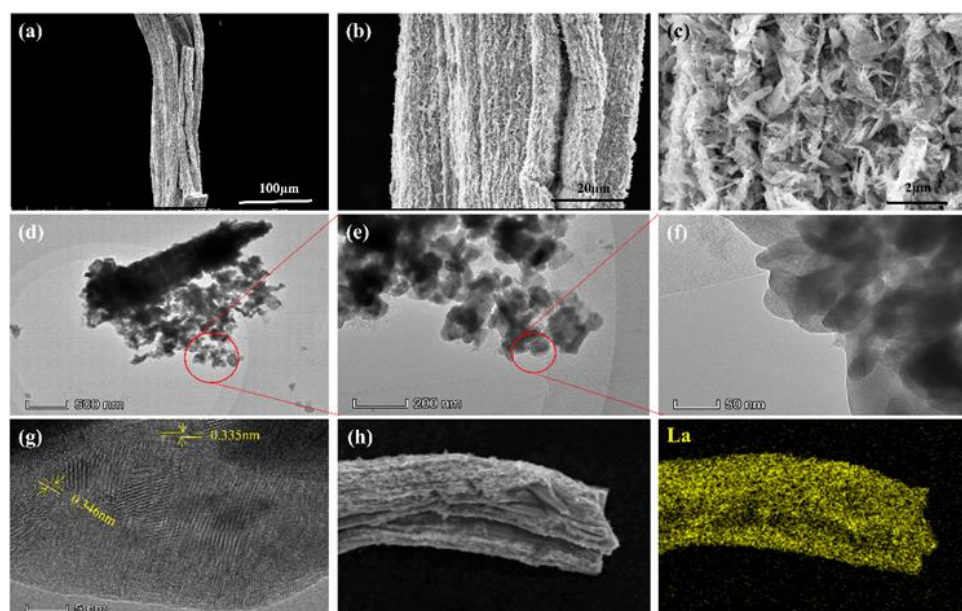


**Figure 1.** (a-c) SEM images of La-BC; (d-g) TEM images of La-BC; (h) elemental mapping images of La-BC.

The XRD patterns of La-BC (900°C) at four different carbonization temperatures are shown in Figure 2. The composition of its elements and substances is analyzed. It can be found that the existence forms of La change with the increase of calcining temperature. For La-BC at 700°C and La-BC at 800°C, there were diffraction peaks of La<sub>2</sub>CO<sub>5</sub> (PDF#23-0320), while for La-BC at 900°C and La-BC at 1000°C, there were characteristic peaks of La<sub>2</sub>O<sub>3</sub> (PDF#05-0602), which proves that La was successfully loaded on the adsorption materials[30] and the lanthanum-containing products were different at different carbonization temperatures.

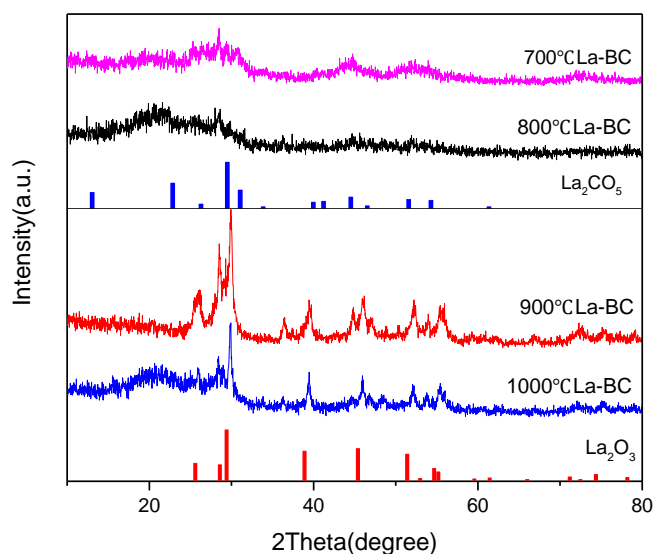


**Figure 2.** XRD patterns of different carbonization temperatures La-BC samples.

In order to further identify the functional groups on La-BC and obtain the possible adsorption mechanism of Cr (VI), the sample La-BC (900°C) was analyzed by X-ray photoelectron spectroscopy (Figure 3). All peaks are calibrated by using C 1s (284.3eV) as a reference. The wide-scan XPS spectrum of La-BC showed that elements C (63.4%) and O (28.96%) were the main components (Figure 3a). The peaks at the binding energy of 835.6 eV, 839.0 eV, 852.6 eV and 855.8 eV confirmed the introduction of La<sup>3+</sup> on the bio-char surface (Figure 3b).

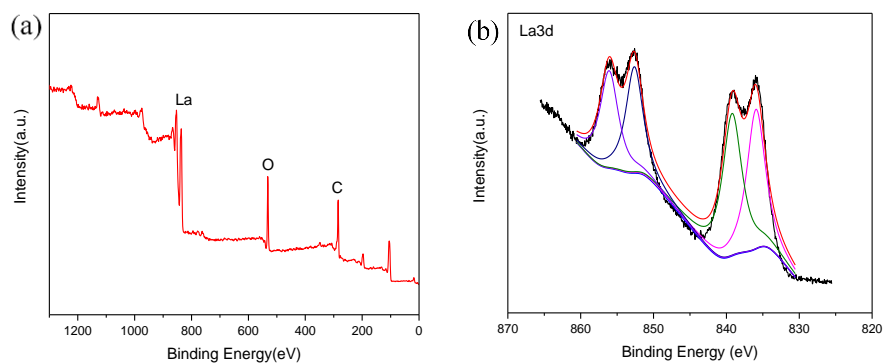


**Figure 3.** (a) XPS spectra of the La-BC (900°C) before Cr (VI) adsorption; (b) La 3d spectra of La-BC (900°C) before Cr (VI) adsorption.

### 3.2. Adsorption isotherm

The adsorption isotherm refers to the relation curve between the adsorption amount of adsorbent and the equilibrium concentration of adsorbent after the adsorption process occurs at the set adsorption temperature. This process can be fitted by the adsorption isotherm model (Text S1). The correlation between Langmuir and Freundlich isotherm models and experimental data with different initial chromium concentrations was studied. The isothermal adsorption model fitting of carbonized La-BC at four temperatures is shown in Figure 4. Under the conditions of pH4.6, 300rpm, 303K, contact time 5h and dosage of adsorbent 1g/L, adsorption experiments were carried out with four kinds of La-BC, in which the range of initial potassium dichromate concentration was from 20 to 1000 mg/L. It was found that the adsorption capacity of La-BC (700°C-1000°C) increased

from 2.2 to 37.6mg/g, 9.6 to 56.3mg/g, 5.8 to 83.5mg/g, and 3.2 to 39.6mg/g, respectively. The increase of the initial concentration of potassium dichromate solution might result in the improvement collisions between La-BC and Cr (VI), as well as increase the driving force of removing Cr (VI), thus promoting adsorption[35]. The adsorption isotherm shows that in the carbonized La-BC at four different temperatures, the adsorption capacity of 900 °C La-BC is higher, which may be attributed to the following two reasons: (1) as the specific surface area and pore size of 900 °C La-BC are larger than those of the other three kinds of La-modified biochar (Table S1), there are more available adsorption sites, enhancing the adsorption capacity of 900 °C La-BC; (2) according to the XRD pattern (Figure 2), the lanthanum compounds loaded with 900 °C La-BC and 1000 °C La-BC was  $\text{La}_2\text{O}_3$ , which could be used as an active adsorption site for metal ions. Langmuir isotherm model showed that the saturated adsorption amounts of Cr (VI) with four kinds of La-BCs respectively were 41.4mg/g, 67.4mg/g, 104.9mg/g and 49.9mg/g (Table S2). The fitting results showed that the adsorption process had consistency with both Langmuir model and Freundlich model, which conformed to the Langmuir model more, suggesting the adsorption process should exist monolayer and multilayer adsorption, especially the adsorption of single molecule layer[35, 36].

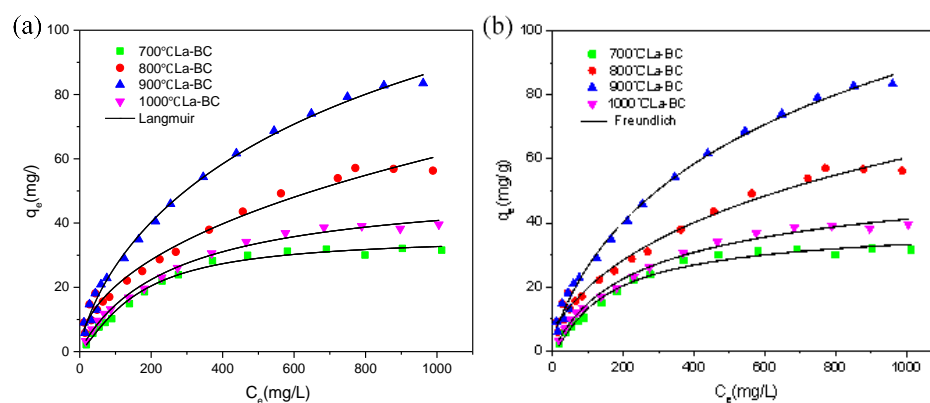


**Figure 4.** Fitting the adsorption data of Cr (VI) on La-BC (900 °C) to (a) Langmuir isotherm; (b) Freundlich isotherm.

### 3.3. Adsorption kinetics

Adsorption is a continuous dynamic process characterized by "external diffusion - internal diffusion". This process can be fitted by the adsorption kinetic model (Text S2.) To evaluate chromate adsorption rates of La-BC, the time-dependent sorption was conducted under the conditions of initial Cr (VI) concentration 200mg/L, pH4.6, 300rpm, 303K, contact time 5h and adsorbent dose 1g/L. The relationship between the adsorption amount of Cr (VI) and time of La-BC carbonized at four temperatures is shown in Figure 5a. The adsorption process can be divided into 3 stages: rapid adsorption stage, slow adsorption stage and adsorption equilibrium stage. In the first 20 minutes, the adsorption reaction of Cr (VI) with La-BC was very rapid. The Cr (VI) adsorption capacity of La-BC (700 °C-1000 °C) was 14.1mg/g, 19.0mg/g, 30.3mg/g and 15.5mg/g, which occupied the corresponding equilibrium adsorption capacity 95.5%, 93.1%, 93.5% and 95.7% respectively, and the adsorption capacity of La-BC at 900 °C was far higher than that of the other three adsorbents. The following 70min is the slow adsorption phase. After 90min, there was no significant difference between the concentration of Cr (VI) and that after 3h in the solvent, showing that the adsorption process entered the equilibrium stage due to the saturation of the sites[1, 37]. The differences between these stages can be explained as follows: (1) at first, the concentration of Cr (VI) at the interface of the adsorbent was the highest, forming a large adsorption dynamic gradient, which drove Cr (VI) occupied the adsorption site on the outer surface of La-BC rapidly; (2) when Cr (VI) entered the inte-

rior of La-BC, the adsorption rate decreased due to the blockage of pores and the decrease of active adsorption sites; (3) with the slow adsorption continued, the adsorption rate gradually decreased until reached the dynamic adsorption equilibrium.

To determine the adsorption mechanism, the equilibrium data were used to fit the pseudo-first-order and pseudo-second-order models (Table S3). The fitting results showed that the pseudo second order kinetic equation can better describe the adsorption behavior. In other words, the adsorption of Cr (VI) on La-BC was closer to chemisorption, which carried out through polar functional groups sharing or exchanging electrons between adsorbate and adsorbent[38, 39].

### 3.4. Adsorption thermodynamics

Temperature is an important factor affecting the adsorption effect. Temperature changes affect the value of thermodynamic parameters (Text S3). Under the conditions of initial Cr (VI) concentration 100-900 mg/L, contact time 5h, pH=4.6, adsorbent 300rpm and dose 1g/L, the relation between the adsorption amount of Cr (VI) with La-BC (900°C) and the adsorption temperature is shown in Figure 5b. The increase of the adsorption temperature makes the adsorption amount increase. The calculated adsorption reaction enthalpy change  $\Delta H$  was 41.66 KJ/mol,  $\Delta S$  was 144.6 J/(mol·K), and gibbs free energy change  $\Delta G < 0$  at each temperature (Table S4), which showed that the adsorption was a spontaneous endothermic reaction, in other word, the rise of temperature led prompt reaction[12, 16, 40].

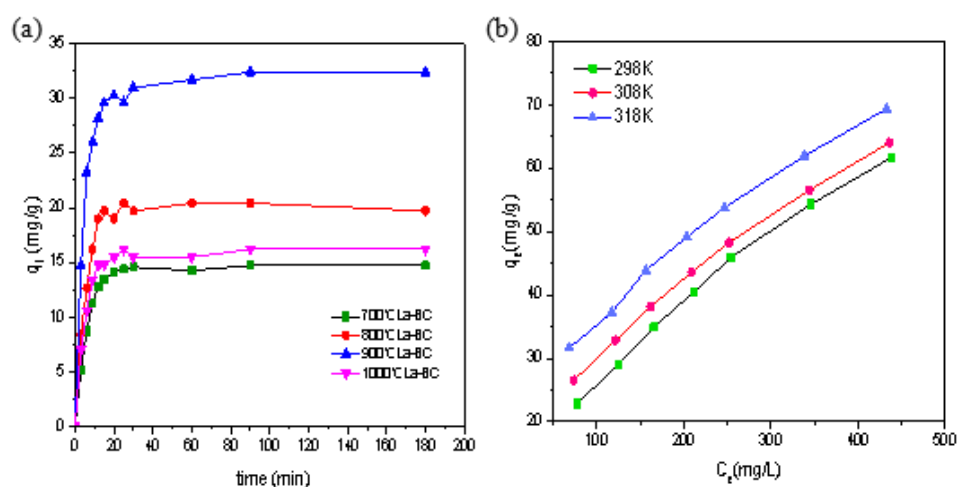
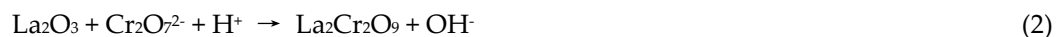


**Figure 5.** (a) Relationship between adsorption amount of Cr (VI) and adsorption time by La-BC at four carbonization temperatures; (b) relationship between adsorption amount of Cr (VI) and adsorption temperature by La-BC (900°C).

### 3.5. Effect of solution pH on adsorption experiment

Under the conditions of initial concentration 250mg/L, 300rpm, 298K, contact time 5h and adsorbent of 1g/L, the effect of pH on adsorption capacity of Cr (VI) with La-BC (900 °C) was shown in Figure 6a, while the comparison of initial and final pH of the solution before and after adsorption was also demonstrated. The selected pH range was 2-10, within which the adsorption capacity of chromate decreased significantly with the increase of pH, and the maximum adsorption capacity was 68.52mg/g, appearing at pH=2. The existence form of chromate is related to the pH of solution. At acidic pH, the main types of chromate existent forms are  $\text{Cr}_2\text{O}_7^{2-}$ ,  $\text{HCrO}_4^-$  and  $\text{CrO}_4^{2-}$ [12, 41]. At the same time, the surface of La loaded biochar is positively charged, therefore, under acidic conditions, the adsorption mechanism of chromate by La-BC may be explained as electrostatic in-

teraction[14, 32]. The change of pH before and after the adsorption proves another possible mechanism: the final pH of the solution was all higher than the initial pH, indicating that  $\text{OH}^-$  was released during the process of chromate adsorption, which confirmed that ligand exchange interaction was involved in[30]. Based on the above, several possible adsorption equations are summarized as follows:



With the increase of pH ( $> \text{pH}_{\text{pzc}}$ ), a large amount of  $\text{OH}^-$  was released into the solution, which can compete with chromate ions for active adsorption sites and generate electrostatic repulsion[23]. All above resulted in a significant decrease adsorption of chromate at a higher pH value, therefore, the range of pH  $> 7$  were no longer taken into account in subsequent experiments.

The XRD images of La-BC ( $900^\circ\text{C}$ ) before and after the adsorption of dichromate solution with a pH range of 2-7 were compared (Figure 6b). The results showed that when pH  $> 2$  the main peaks after adsorption were characteristic peaks of  $\text{La}(\text{OH})_3$  (PDF#36-1481). When pH=2, the XRD image of La-BC was a smooth curve without any peak. The reason may be that  $\text{La}_2\text{O}_3$  in La-BC ( $900^\circ\text{C}$ ) was largely dissolved into the solution under a strong acidic environment. For this reason, the amount of La dissolution of the adsorbed dichromate solution was detected (Figure S2), and the results confirmed that a large amount of La was dissolved at pH=2. The initial pH of dichromate solution is about 4-5, within this range, not only can the adsorption amount of La-BC be guaranteed not to be too low, but also the dissolution amount of La can be kept at a low level. Based on the results of all parties, it is finally decided that the experiment will not make too much adjustment to the pH of the initial solution and keep it at pH=4.6.

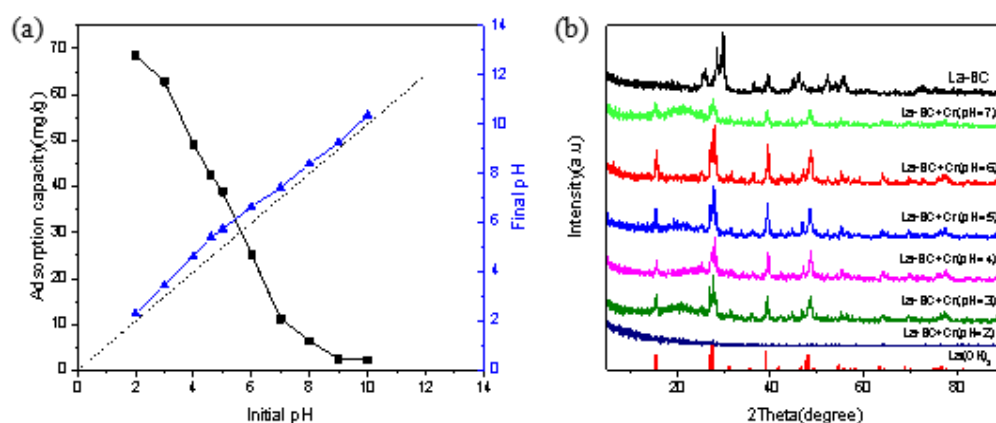


**Figure 6.** (a) The effect of pH on adsorption amount and the comparison of initial and final pH; (b) the XRD images of La-BC ( $900^\circ\text{C}$ ) after adsorption when pH at the range of 2-7.

### 3.6. Effect of coexisting acid ions on adsorption experiments

Five kinds of 100mg/L  $\text{K}_2\text{Cr}_2\text{O}_7$  solutions which contained  $\text{NaCl}$ ,  $\text{Na}_2\text{SO}_4$ ,  $\text{NaNO}_3$ ,  $\text{NaHCO}_3$  and  $\text{Na}_2\text{HPO}_4$  were prepared, in which the concentration of coexisting ions was 0.05mol/L, 0.1mol/L and 0.2mol/L, respectively. The pure 100mg/L  $\text{K}_2\text{Cr}_2\text{O}_7$  was used as a blank control, and adsorption experiments were carried out under the conditions of 300rpm, 303K, contact time 5h, pH 4.6 and 1g/L dosage of La-BC ( $900^\circ\text{C}$ ). It was showed

that different interfering ions had different influence on the adsorption amount of Cr (VI) (Figure 7a). The results explained that  $\text{Cl}^-$  and  $\text{NO}_3^-$  had no effect on the adsorption of chromate and  $\text{SO}_4^{2-}$  had little effect. However,  $\text{HCO}_3^-$  and  $\text{HPO}_4^{2-}$  seriously interfered the adsorption of chromate, which may be stated by the following two reasons: (1) the structure of these oxygen-containing acid groups was similar to that of  $\text{Cr}_2\text{O}_7^{2-}$  and  $\text{CrO}_4^{2-}$ , resulting in the competition in the adsorption process; (2) both carbonic acid and phosphoric acid are weak acids, so the hydrolysis degree of  $\text{HCO}_3^-$  and  $\text{HPO}_4^{2-}$  in the solution is greater than the degree of ionization -- that is why  $\text{NaHCO}_3$  and  $\text{Na}_2\text{HPO}_4$  solutions are weakly alkaline. The release of  $\text{OH}^-$  led to the decrease of the adsorption amount of chromate.

### 3.7. Cycle experiments

The experiment of adsorption of Cr(VI) by La-BC(900°C) was carried out under the conditions of initial Cr (VI) concentration 200mg/L, pH4.6, 300rpm, 303K, contact time 5h and adsorbent dosage 1g/L, and five cycles were carried out by the desorption treatment of 1mol/L NaOH (Figure 7b). After each cycle, the recovered product was calcined in inert gas at high temperature to ensure that the composition of the recovered product is the same as the original La-BC material. The experimental results showed that La-BC(900°C) had good stability, low loss in five cycles and good reuse effect. The circulating experiment also proved the possibility of La-BC widely used in treating chromium-containing wastewater.

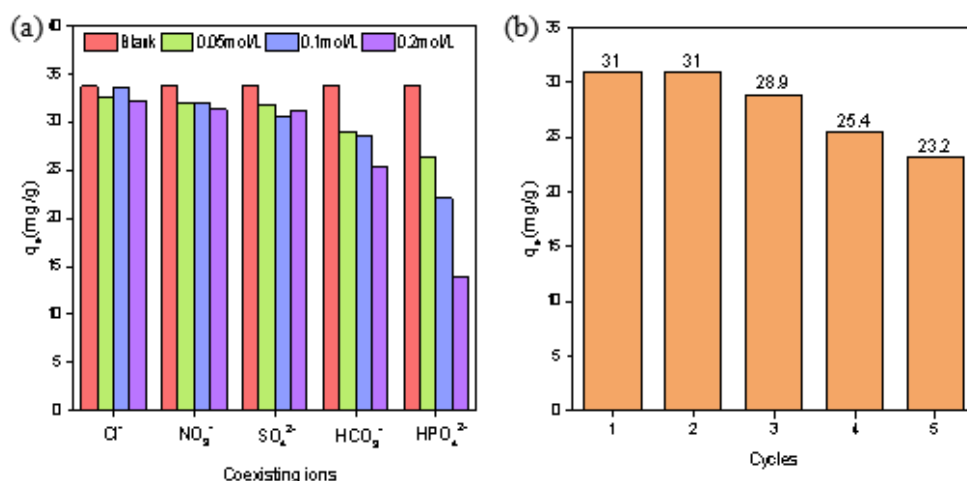


**Figure 7.** (a) Effect of coexisting ions on the adsorption amount of Cr (VI); (b) five cycles of Cr (VI) adsorption by La-BC (900°C).

### 3.8. Adsorption mechanism

PH experiments and XRD characterization results indicated that the adsorption behavior of La-BC on Cr (VI) might have electrostatic interaction and ligand exchange (Figure 7). In addition, X-ray photoelectron spectroscopy analysis was performed on La-BC (900°C) after adsorption of chromite, and comparison was made with XPS image of La-BC (900°C) before adsorption (Figure 8). The wide-scan XPS spectrum of La-BC after experiments showed that the peak of Cr element has appeared in La-BC (900°C) (Figure 8a). Moreover, the corresponding peaks where the binding capacity was 577.8 eV, 579.7 eV proved that Cr(VI) were successfully absorbed (Figure 8b)[42]. Cr has been absorbed successfully, In the La3d images, the binding energy of element La had negative displacement (0.4-0.7eV) after adsorption (Figure 8c), indicating that electron transfer occurred between La-BC (900°C) and chromite, which formed a strong chemical bond[30]. The O1s spectrum changed significantly before and after adsorption, which could explain the adsorption mechanism (Figure 8d and e). O1s deconvolution (Figure 8d) indicated, three main oxygen components -- lattice oxygen La-O (530.8eV), -OH

(531.9eV), and adsorbed H<sub>2</sub>O (533.0eV) -- existed in La-BC. But after Cr (VI) sorption, the peak of La-O was nearly disappeared while H<sub>2</sub>O percentage increased (Figure 8e). It was because La<sub>2</sub>O<sub>3</sub> was hygroscopic and adsorbed moisture to become La (OH)<sub>3</sub> [28]. All above results show that the adsorption may be caused by ligand exchange or complexation. The increase of the proportion of element O from 28.96% to 32.47% might also be explained by the adsorption of oxygen-containing acid radical CrO<sub>4</sub><sup>2-</sup> and Cr<sub>2</sub>O<sub>7</sub><sup>2-</sup>.

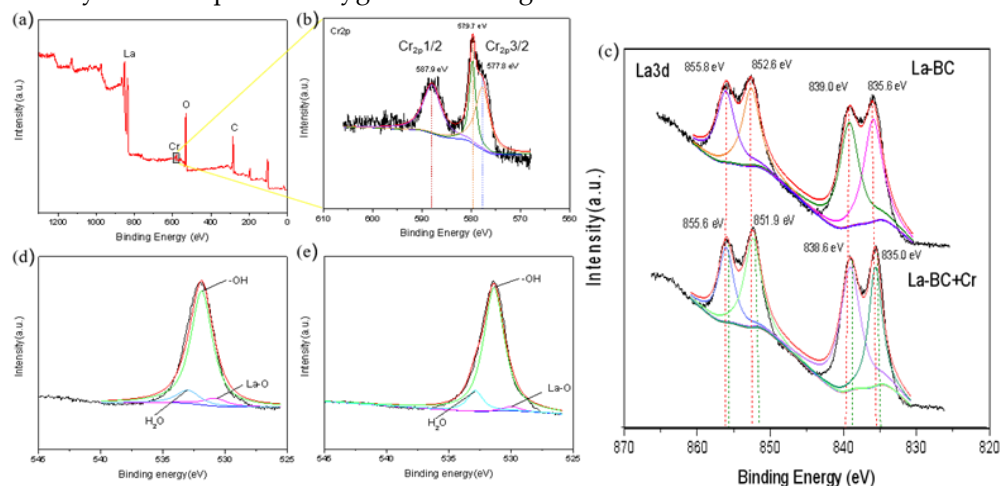


**Figure 8.** (a) XPS spectra of the La-BC (900°C) after Cr (VI) adsorption(a); (b) Cr2p; (c) La3d; (d) O1s spectra of La-BC (900°C) before and (e) after Cr (VI) adsorption.

#### 4. Conclusions

**Table 1.** Literature data on the adsorption of Cr (VI) ions by various adsorbent.

Adsorbent	Adsorption capacity(mg/g)	Ref.
MgAl-LDH	84.2	[42]
MWCNTs-70	17.2	[15]
Chitosan engraved iron and lanthanum mixed oxyhydroxide	106.04	[32]
Fe <sub>3</sub> O <sub>4</sub> nanoparticles functionalized poly-vinyl alcohol/chitosan magnetic composite hydrogel	24.69	[43]
Chitosan-citric acid nanoparticles	106.15	[44]
Cross-linked chitosan bentonite composite	89.13	[45]
Fe-Mn oxide-modified biochar	59.8	[16]
Biochar supported nZVI composite	31.53	[1]
La <sub>2</sub> O <sub>3</sub> -dropped biochar	104.9	This article

In this experiment, wet spinning and ion exchange were combined to load La<sup>3+</sup> onto sodium alginate fiber, and then La<sup>3+</sup> was converted to La<sub>2</sub>O<sub>3</sub> in the process of high-temperature carbonization. Lanthanum oxide modified biochar showed excellent adsorption capacity for chromate, and it also had a high adsorption capacity in potassium dichromate solution with high concentration at room temperature, and its saturated adsorption capacity was about 104.9mg/g. The isotherm data show that the adsorption process is more consistent with Langmuir model and has a higher correlation with the adsorption of single molecular layer. The adsorption kinetic data followed the pseudo-second-order kinetic model, showing that the adsorption process was dominated by

chemisorption. The thermodynamic parameters prove that the adsorption of chromate by La-BC is spontaneous and endothermic. In addition to physical adsorption, the adsorption mechanism of Cr (VI) in La-BC may be electrostatic interaction, ligand exchange or complexation (Figure 9). Compared with Cr (VI) adsorbents in other literatures (Table 1), La-BC has the advantages of large adsorption capacity, simple preparation process and good recycling performance. Therefore, La-BC can be used as a new type of environmentally friendly adsorbent, which has great research significance and broad development prospect in the field of sewage treatment.

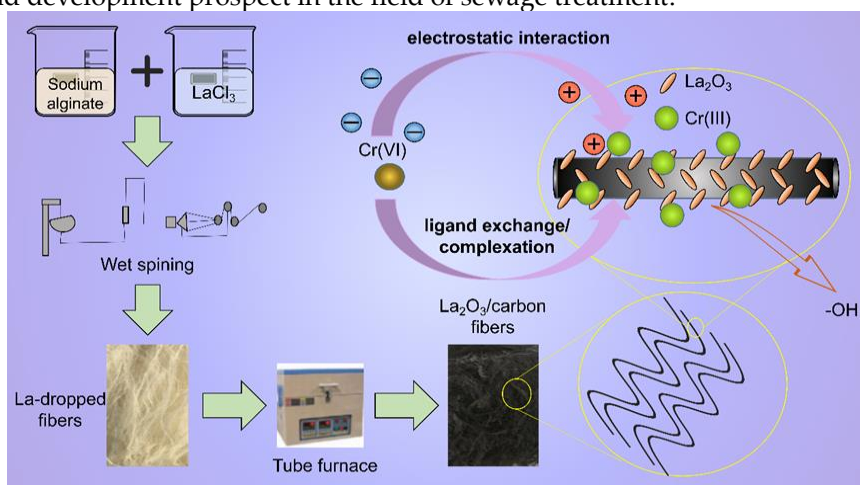


Figure 9. Preparation process of La-BC and mechanism of Cr (VI) adsorption with it

#### Supplementary Materials:

##### Text S1. Langmuir and Freundlich isotherm model

$$\text{Langmuir adsorption isothermal model: } \frac{C_e}{q_e} = \frac{C_e}{q_m} + \frac{1}{b q_m}, \quad (4)$$

$$\text{Freundlich adsorption isothermal model: } \log q_e = \frac{1}{n} \log C_e + \log K_f, \quad (5)$$

Where  $q_e$  (mg/g) represents the adsorption amount of adsorbents per unit adsorbent at adsorption equilibrium,  $C_e$  (mg/L) represents the concentration of adsorbents at adsorption equilibrium,  $q_m$  (mg/g) represents the maximum adsorption capacity of adsorbents, and  $b$  represents the adsorption coefficient and the affinity strength between adsorbents and adsorbents. In addition,  $K_f$  is the adsorption capacity constant, indicating the adsorption capacity of the adsorbent. The  $n$  value may reflect the heterogeneity of the adsorbent or the adsorption reaction strength.

##### Text S2. Pseudo-first and pseudo-second order kinetic model

$$\text{Pseudo-first order kinetic equation: } \ln(q_e - q_t) = \ln q_e - k_1 t, \quad (6)$$

$$\text{Pseudo-second order kinetic equation: } \frac{t}{q_t} = \frac{1}{k_2 q_e^2} + \frac{t}{q_e}, \quad (7)$$

Where  $q_e$  and  $q_t$  (mg/g) are the amount of Cr (VI) adsorbed on the adsorbent at equilibrium and at any time  $t$  (min), respectively.  $k_1$  and  $k_2$  are the separate rate constants for pseudo first-order and pseudo second-order sorption model.

##### Text S3. Adsorption thermodynamics

$$\text{Thermodynamic formula: } \ln K_D = \frac{\Delta S}{R} - \frac{\Delta H}{RT}, \quad (8)$$

The thermodynamic parameter of adsorption is the gibbs free energy change ( $\Delta G$ ,  $\text{kJ}\cdot\text{mol}^{-1}$ )、enthalpy change ( $\Delta H$ ,  $\text{kJ}\cdot\text{mol}^{-1}$ ) and the entropy change ( $\Delta S$ ,  $\text{J}\cdot\text{mol}^{-1}\cdot\text{K}^{-1}$ ). The thermodynamic equation of adsorption reaction reflects the change of adsorption heat and temperature.  $R$  represents the ideal gas constant, whose value is  $8.314 \text{ J}\cdot\text{mol}^{-1}\cdot\text{K}^{-1}$ ;  $T$  is the thermodynamic temperature

(K);  $K_D$  ( $L \cdot g^{-1}$ ) represents the adsorption equilibrium constant, which can be calculated by the Freundlich model.

The linear fitting of  $\ln K_D$  and  $1/T$  resulted in a line, and the enthalpy and entropy changes of the adsorption reaction were calculated by its slope and intercept. In general, if  $\Delta G < 0$ , the adsorption reaction is spontaneous, if  $\Delta G > 0$ , it is a spontaneous reaction, can undertake the reverse; If  $\Delta H > 0$ , the adsorption reaction is endothermic reaction, if  $\Delta H < 0$ , the adsorption reaction is exothermic reaction; If  $\Delta S > 0$ , that is, the adsorption reaction of entropy, said confusion degree increased adsorption system, is advantageous to the reaction of spontaneous.

**Table S1** Physical properties of different samples

Samples	Surface area( $m^2/g$ )		Pore volume( $cm^3/g$ )		$D_p$ (nm)
	$S_{BET}$	$V_{total}$	$V_{micro}$		
700°C La-BC	8.21	0.0037	0.0169		10.9198
800°C La-BC	38.61	0.0328	0.0196		4.0095
900°C La-BC	177.41	0.2515	0.0803		6.2749
1000°C La-BC	52.08	0.0547	0.0255		5.2147

**Table S2** Parameters of Cr (VI) adsorption isotherms based on Freundlich and Langmuir models.

Materials	Langmuir model			Freundlich model		
	$q_m$ (mg/g)	$b$ (L/mg)	$R^2$	$K_f$	$n$	$R^2$
700°C La-BC	41.4	0.0041	0.976	0.505	1.543	0.929
800°C La-BC	67.4	0.0049	0.953	2.255	2.098	0.950
900°C La-BC	104.9	0.0037	0.962	1.715	1.716	0.964
1000°C La-BC	49.9	0.0042	0.994	0.776	1.655	0.963

**Table S3** Parameters of Cr (VI) adsorption kinetics based on pseudo-first-order and pseudo-second-order dynamic models

Materials	Pseudo-first-order model			Pseudo-second-order model		
	$q_e$ (mg/g)	$K_1 \times 10^{-2}$	$R^2$	$q_e$ (mg/g)	$K_2 \times 10^{-2}$	$R^2$
700°C La-BC	14.3	15.19	0.9944	14.26	0.95	0.9880
800°C La-BC	20.4	24.51	0.9696	20.42	0.40	0.9880
900°C La-BC	32.4	10.96	0.9698	32.39	1.33	0.9998
1000°C La-BC	15.5	15.21	0.9428	15.49	2.94	0.9995

**Table S4** Thermodynamic parameters for chromate adsorption with La-BC(900°C)

Temperature (K)	Thermodynamic parameters		
	$\Delta H$ (KJ/mol)	$\Delta S$ (J/(mol·K))	$\Delta G$ (KJ/mol)
298	41.66	144.6	-1.44
308			-2.78
318			-4.059

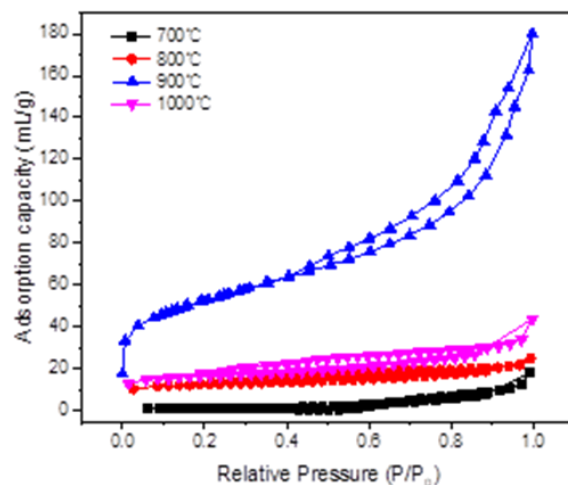


Figure S1. Nitrogen adsorption/desorption isotherms for different samples.

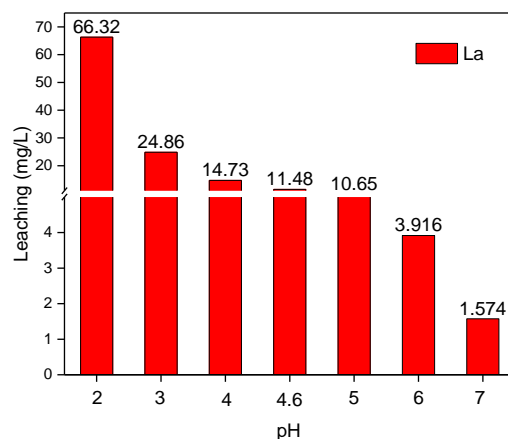


Figure S2. The leaching rate of lanthanum when pH at the range of 2-7.

**Author Contributions:** Conceptualization, X.S. and Y.S.; methodology, X.S. and Y.S.; investigation, X.S. and Y.S.; software, X.S.; validation, X.S.; formal analysis, X.S., Y.S. and Y.C.; resources, P.G., Y.S. and Y.C.; data curation, X.S. and P.G.; writing original draft preparation, X.S.; writing review and editing, X.S., P.G., Y.S. and Y.C.; supervision, Y.S. and Y.C.; project administration, Y.C. All authors have read and agreed to the published version of the manuscript.

**Funding:** This research was funded by Science and Technology Support Plan for Youth Innovation of Colleges in Shandong Province (DC200000961), China Geological Survey (Grant DD20189503) and the Natural Science Foundation of Shandong Province, China (No. ZR2019BF031).

**Acknowledgments:** Science and Technology Support Plan for Youth Innovation of Colleges in Shandong Province (DC200000961), China Geological Survey (Grant DD20189503) and the Natural Science Foundation of Shandong Province, China (No. ZR2019BF031) were acknowledged for supporting this work.

**Conflicts of Interest:** The authors declare no conflict of interest. The funders had no role in the design of the study; in the collection, analyses, or interpretation of data; in the writing of the manuscript, or in the decision to publish the results.

## References

1. Fan, Z., et al., *Removal of hexavalent chromium by biochar supported nZVI composite: Batch and fixed-bed column evaluations, mechanisms, and secondary contamination prevention*. Chemosphere, 2019. **217**: p. 85-94.
2. Lyu, H., et al., *Removal of hexavalent chromium from aqueous solutions by a novel biochar supported nanoscale iron sulfide composite*. Chemical Engineering Journal, 2017. **322**: p. 516-524.
3. Shi, S., et al., *Enhanced Cr(VI) removal from acidic solutions using biochar modified by Fe<sub>3</sub>O<sub>4</sub>@SiO<sub>2</sub>-NH<sub>2</sub> particles*. Sci Total Environ, 2018. **628-629**: p. 499-508.
4. Helz, R.J.K.a.G.R., *Indirect photoreduction of aqueous chromium(VI)*. Environ. Sci. Technol., 1992. **1992**, **26**, **307-312**.
5. Fu, H., et al., *Dissolved Mineral Ash Generated by Vegetation Fire Is Photoactive under the Solar Spectrum*. Environ Sci Technol, 2018. **52**(18): p. 10453-10461.
6. Hausladen, D.M., et al., *Hexavalent Chromium Sources and Distribution in California Groundwater*. Environmental Science & Technology, 2018. **52**(15): p. 8242-8251.
7. Zhang, W., et al., *Simultaneous redox conversion and sequestration of chromate(VI) and arsenite(III) by iron(III)-alginate based photocatalysis*. Applied Catalysis B: Environmental, 2019. **259**.
8. Liu, T., et al., *Entrapment of nanoscale zero-valent iron in chitosan beads for hexavalent chromium removal from wastewater*. J Hazard Mater, 2010. **184**(1-3): p. 724-30.
9. *Guidelines for Drinking Water Quality 2011*.
10. Anhuai Lu, S.Z., Jie Chen, Junxian Shi, Junli Tang, and Xiaoying Lu, *Removal of Cr(VI) and Cr(III) from Aqueous Solutions and Industrial Wastewaters by Natural Clino-pyrrhotite*. Environmental Science & Technology.
11. ZHIHUI AI, YING CHENG, LIZHI ZHANG, a.J.Q., *Efficient Removal of Cr(VI) from Aqueous Solution with Fe@Fe<sub>2</sub>O<sub>3</sub> Core-Shell Nanowires*. Environmental Science & Technology, 2008.
12. Ajmani, A., et al., *Hexavalent chromium adsorption on virgin, biochar, and chemically modified carbons prepared from Phanera vahlii fruit biomass: equilibrium, kinetics, and thermodynamics approach*. Environ Sci Pollut Res Int, 2019. **26**(31): p. 32137-32150.
13. Li, Y., et al., *Efficient removal of As(III) from aqueous solution by S-doped copper-lanthanum bimetallic oxides: Simultaneous oxidation and adsorption*. Chemical Engineering Journal, 2020. **384**.
14. Siddiqui, M.F. and T.A. Khan, *Gelatin-polyvinyl alcohol/lanthanum oxide composite: A novel adsorbent for sequestration of arsenic species from aqueous environment*. Journal of Water Process Engineering, 2020. **34**.
15. Peng, Y., et al., *Adsorption of Chromate from Aqueous Solution by Polyethylenimine Modified Multi-Walled Carbon Nanotubes*. J Nanosci Nanotechnol, 2018. **18**(6): p. 4006-4013.
16. Wang, B., F. Li, and L. Wang, *Enhanced hexavalent chromium (Cr(VI)) removal from aqueous solution by Fe-Mn oxide-modified cattail biochar: adsorption characteristics and mechanism*. Chemistry and Ecology, 2019. **36**(2): p. 138-154.
17. Yin, Z., et al., *A novel magnetic biochar prepared by K<sub>2</sub>FeO<sub>4</sub>-promoted oxidative pyrolysis of pomelo peel for adsorption of hexavalent chromium*. Bioresour Technol, 2020. **300**: p. 122680.
18. Gupta, V.K., S. Agarwal, and T.A. Saleh, *Chromium removal by combining the magnetic properties of iron oxide with adsorption properties of carbon nanotubes*. Water Res, 2011. **45**(6): p. 2207-12.
19. Inyang, M.I., et al., *A review of biochar as a low-cost adsorbent for aqueous heavy metal removal*. Critical Reviews in Environmental Science and Technology, 2015. **46**(4): p. 406-433.
20. Li, H., et al., *Mechanisms of metal sorption by biochars: Biochar characteristics and modifications*. Chemosphere, 2017. **178**: p. 466-478.

21. Wang, L., et al., *Enhanced antimonate (Sb(V)) removal from aqueous solution by La-doped magnetic biochars*. Chemical Engineering Journal, 2018. **354**: p. 623-632.
22. Koilraj, P. and K. Sasaki, *Selective removal of phosphate using La-porous carbon composites from aqueous solutions: Batch and column studies*. Chemical Engineering Journal, 2017. **317**: p. 1059-1068.
23. Yang, B., et al., *Lanthanum ferrite nanoparticles modification onto biochar: derivation from four different methods and high performance for phosphate adsorption*. Environmental Science and Pollution Research, 2019. **26**(21): p. 22010-22020.
24. Yang, H., et al., *Removal of Arsenate and Chromate by Lanthanum-modified Granular Ceramic Material: The Critical Role of Coating Temperature*. Sci Rep, 2019. **9**(1): p. 7690.
25. Catalano, J.G., et al., *Simultaneous inner- and outer-sphere arsenate adsorption on corundum and hematite*. Geochimica et Cosmochimica Acta, 2008. **72**(8): p. 1986-2004.
26. Liao, T., et al., *La(OH)<sub>3</sub>-modified magnetic pineapple biochar as novel adsorbents for efficient phosphate removal*. Bioresour Technol, 2018. **263**: p. 207-213.
27. Lin, L., et al., *Enhanced As(III) removal from aqueous solution by Fe-Mn-La-impregnated biochar composites*. Sci Total Environ, 2019. **686**: p. 1185-1193.
28. Chen, C., et al., *Simultaneous removal of butylparaben and arsenite by MOF-derived porous carbon coated lanthanum oxide: Combination of persulfate activation and adsorption*. Chemical Engineering Journal, 2020. **391**.
29. Li, X., et al., *Interactions of phosphate and dissolved organic carbon with lanthanum modified bentonite: Implications for the inactivation of phosphorus in lakes*. Water Res, 2020. **181**: p. 115941.
30. Shan, S., et al., *Remarkable phosphate removal and recovery from wastewater by magnetically recyclable La<sub>2</sub>O<sub>2</sub>CO<sub>3</sub>/gamma-Fe<sub>2</sub>O<sub>3</sub> nanocomposites*. J Hazard Mater, 2020. **397**: p. 122597.
31. Zhong, Z., et al., *Phosphate sequestration by magnetic La-impregnated bentonite granules: A combined experimental and DFT study*. Sci Total Environ, 2020. **738**: p. 139636.
32. Preethi, J., S. Vigneshwaran, and S. Meenakshi, *Performance of chitosan engraved iron and lanthanum mixed oxyhydroxide for the detoxification of hexavalent chromium*. Int J Biol Macromol, 2019. **130**: p. 491-498.
33. Xing, Y., et al., *Direct electrospun La<sub>2</sub>O<sub>3</sub> nanowires decorated with metal particles: Novel 1 D adsorbents for rapid removal of dyes in wastewater*. Journal of Materials Science & Technology, 2020. **45**: p. 84-91.
34. Andrey Bagreev, T.J.B., David C. Locke, *Pore structure and surface chemistry of adsorbents obtained by pyrolysis of sewage sludge-derived fertilizer*. Carbon, 2001. **39** (2001) **1971-1979**.
35. Moussavi, G. and B. Barikbin, *Biosorption of chromium(VI) from industrial wastewater onto pistachio hull waste biomass*. Chemical Engineering Journal, 2010. **162**(3): p. 893-900.
36. Gupta, V.K. and A. Rastogi, *Biosorption of hexavalent chromium by raw and acid-treated green alga Oedogonium hatei from aqueous solutions*. J Hazard Mater, 2009. **163**(1): p. 396-402.
37. Liang, J., et al., *Amorphous MnO<sub>2</sub> Modified Biochar Derived from Aerobically Composted Swine Manure for Adsorption of Pb(II) and Cd(II)*. ACS Sustainable Chemistry & Engineering, 2017. **5**(6): p. 5049-5058.
38. Y.S. Ho, G.M., *Pseudo-second-order model for sorption processes*. Process Biochemistry 1999. **34** (1999) **451-465**.
39. Zhang, X., L. Zhang, and A. Li, *Eucalyptus sawdust derived biochar generated by combining the hydrothermal carbonization and low concentration KOH modification for hexavalent chromium removal*. J Environ Manage, 2018. **206**: p. 989-998.
40. You, N., et al., *Synergistic removal of arsenic acid using adsorption and magnetic separation technique based on Fe<sub>3</sub>O<sub>4</sub>@ graphene nanocomposite*. Journal of Industrial and Engineering Chemistry, 2019. **70**: p. 346-354.
41. Labied, R., et al., *Adsorption of hexavalent chromium by activated carbon obtained from a waste lignocellulosic material (Ziziphus jujubacores): Kinetic, equilibrium, and thermodynamic study*. Adsorption Science & Technology, 2018. **36**(3-4): p. 1066-1099.
42. Koilraj, P. and K. Sasaki, *Eco-Friendly Alkali-Free Arginine-Assisted Hydrothermal Synthesis of Different Layered Double Hydroxides and Their Chromate Adsorption/Reduction Efficiency*. ChemistrySelect, 2017. **2**(32): p. 10459-10469.

- 
43. Yan, E., et al., *Synthesis of Fe<sub>3</sub>O<sub>4</sub> nanoparticles functionalized polyvinyl alcohol/chitosan magnetic composite hydrogel as an efficient adsorbent for chromium (VI) removal*. Journal of Physics and Chemistry of Solids, 2018. **121**: p. 102-109.
  44. Bagheri, M., et al., *Application of chitosan-citric acid nanoparticles for removal of chromium (VI)*. Int J Biol Macromol, 2015. **80**: p. 431-44.
  45. Liu, Q., et al., *Adsorptive removal of Cr(VI) from aqueous solutions by cross-linked chitosan/bentonite composite*. Korean Journal of Chemical Engineering, 2015. **32**(7): p. 1314-1322.